DR. BRANDON T HASSETT (Orcid ID : 0000-0002-1715-3770)

Hassett & Gardinger---Aplanochytrid Emendment and New Species of Thraustochytrid

New Species of Saprobic Labyrinthulea (=Labyrinthulomycota) and the Erection of a Gen. Nov. to Resolve Molecular Polyphyly within the Aplanochytrids

Brandon T. Hassett[a] and R. Gradinger[a]

a UiT Norges arktiske universtiet, BFE, NFH bygget, Framstredet 6, 9019 Tromsø, Norway

Corresponding author: B Hassett, UiT Norges arktiske universtiet, BFE, NFH bygget, Framstredet 6, 9019 Tromsø, Norway
Telephone: +4777645711; Fax: + 19077824461; E-mail: brandon.hassett@uit.no

ABSTRACT A culture of an unknown unicellular heterotrophic eukaryote was established from pollen-baited seawater acquired from the nearshore environment in proximity to Tromsø, Norway. Light microscopy revealed the production of ectoplasmic nets and reproduction by biflagellate zoospore release, as well as binary division. After culturing and nucleotide extraction, database queries of the isolate's 18S small ribosomal subunit revealed closest affinity to *Aplanochytrium haliotidis*, a pathogen of abalone. Testing of phylogenetic hypotheses consistently grouped our unknown isolate and *A. haliotidis* among the homoplasious thraustochytrids. Transmission electron microscopy revealed complex cell walls comprised of electron-dense lamella that formed protuberances, some associated with bothrosomes. Co-culturing experiments with the marine fungus *Penicillium brevicompactum* revealed prolonged interactions with hyphal strands. Based on the combined information acquired from electron microscopy, life history information, and phylogenetic testing, we describe our unknown isolate as a novel species. To resolve molecular polyphyly within the aplanochytrids, we erect a gen. nov. that circumscribes our novel isolate and the former *A. haliotidis* within the thraustochytrids.

Keywords: 18S rRNA; pollen baiting, homoplasia; Norwegian Sea, thraustochytrid

THE Labyrinthulea (=Labyrinthulomycota) are cosmopolitan heterotrophs that behave as bacteriovores, saprotrophs, and symbionts in marine and freshwater ecosystems. Members of the Labyrinthulea are important decomposers of the detritus pool and whose abundance can exceed 10^3 cells per liter (Ueda et al. 2015). Members of the Labyrinthulea are morphologically distinct from other unicellular heterotrophic eukaryotes by the formation of an ectoplasmic net (Tsui et al. 2009) that is used to interface nutrient acquisition and motility (Bennett et al. 2017). Historically, the Labyrinthulea have been divided into three distinct groups of morphologically-defined taxa: the labyrinthulids that form spindle-shaped vegetative cells enrobed by an ectoplasmic net; thraustochytrids that form a unilateral non-

motile ectoplasmic net; and the aplanochytrids that use gliding motility with an ectoplasmic net (Leander et al. 2004). Phenotypic plasticity within these subgroups hinder the use of morphological characteristics for species identification (Damare & Raghukumar 2006; Leander et al. 2004); consequently, DNA sequences of the 18S small ribosomal subunit (SSU-rRNA) coding region have been used as a diagnostic tool to circumscribe novel clades (Yokoyama et al. 2007; Yokoyama & Honda 2007; FioRito et al. 2016) and guide Labyrinthulea systematics (Leander & Porter 2000).

The taxonomic genus *Aplanochytrium* is morphologically-typed as having a monocentric eucarpic thallus that produces aplanospores which are released by a rupture of the sporangium wall (Bahnweg & Sparrow 1974). There are currently nine described aplanochytrids (Moro et al. 2003; FioRito et al. 2016) that differentially produce zoospores and ectoplasmic nets; yet, are morphologically congruent in the production of aplanospores. Molecular analysis of the 18S SSU-rRNA of these nine species suggests a polyphyletic clade involving *Aplanochytrium haliotidis* (Bongiorni et al. 2005; FioRito et al. 2016), whose molecular sequence has been suggested to be derived from a thraustochytrid contaminant (Leander & Porter 2001) and has been subsequently excluded from molecular phylogenies of the aplanochytrids (e.g. Moro et al. 2003).

We investigated the presence and diversity of the free-living Labyrinthulea in the nearshore Norwegian Sea near Tromsø, Norway using pollen baiting techniques. Analysis of our unicellular isolate revealed closest molecular affinity to *A. haliotidis*. Light and electron microscopy examination of our isolate revealed a similar life history and ultrastructural characteristics as *A. haliotidis*. Phylogenetic analysis of 18S SSU-rRNA sequences places our isolate among the diverse and homoplasious thraustochytrids, forming a clade with *A. haliotidis* that branches sister to uncharacterized isolates from Japan. Based on molecular data, ultrastructure, and life history, we describe our new isolate as a new species, *Labyrinthulochytrium arktikum* (sp. nov.). To begin forming robust phylogenetic hypotheses of thraustochytrid evolution, we use molecular evidence and life history information to erect *Labyrinthulochytrium* (gen. nov.) that circumscribes *Aplanochytrium haliotidis* and *Labyrinthulochytrium arktikum*.

MATERIALS AND METHODS

Isolation and culture

A seawater sample was collected from the nearshore marine environment outside of Tromsø, Norway (N69.663 E18.906) on 22 May 2017. Seawater salinity was measured in the lab using a temperature/salinity probe (YSI, Yellow Springs, OH, USA). Water samples were baited with *Pinus* sp. (Pine) pollen for 3-days at room temperature. Pollen containing fungal-like organisms was drop-streaked onto PmTG media containing 1g peptonized milk, 1g tryptone, 5g glucose, 20g agar (Sigma-Aldrich, St. Louis, MO, USA) liter^{-1} of artificial seawater (Instant Ocean, Blacksburg, VA, USA) adjusted to a salinity of 33 and amended with streptomycin sulfate (500 mg/L) and penicillin G (200 mg/L) antibiotics. Plates were examined after 24 hours and fungal-like isolates were harvested and repeatedly subcultured from a single cell on PmTG agar medium. Axenic cultures were maintained in PmTG broth in 300mL culture flasks at 4°C for life history characterization and molecular analysis. Co-culturing of our isolate with the alga *Chaetoceros socialis* and the marine fungus *Penicillium brevicompactum* was conducted at room temperature for 24 hours and 72 hours, respectively and examined for putative ecological roles.

Morphology and substrate utilization

Cultures were examined and video-recorded for one week following broth inoculation. Cell morphology and life history was viewed using light microscopy on a Leitz DM IL inverted phase contrast microscope. Video was acquired using a fixed microscope adapter with eyepiece camera (AmScope) at 40x magnification with long range objectives.

DNA extraction, amplification, and sequencing

Genomic DNA was isolated from 14-day cell cultures using the DNeasy PowerSoil Kit (Qiagen, Hilden, Germany) following the manufacturer's protocol. Genomic DNA was amplified using polymerase chain reaction (PCR) with Platinum Taq (Life Sciences) and the 18S rRNA NS1/NS4 (5' - GTAGTCATATGCTTGTCTC-3'/5' - CTTCCGTCAATTCCTTTAAG -3') and NS5/NS8 (5' - AACTTAAAGGAATTGACGGAAG-3'/5' - TCCGCAGGTTCACCTACGGA-3') primer pairs (White et al. 1990), as previously described (Hassett et al. 2015). PCR products were purified using the PureLink Quick PCR Purification Kit (Thermo Fisher Scientific) and Sanger sequenced bidirectionally to maximize confidence in base calls along the length of the amplicon. Sanger sequencing was conducted with the BigDye v3.1 Cycle Sequencing Kit (Thermo Fisher Scientific, Waltham, MA, USA) and cycled following the company's recommendations. The sequence reactions were purified using Agencourt's CleanSEQ (Beckman Coulter, Indianapolis, IN, USA) following the company's recommendations. The sequence reactions were resolved using the Applied Biosystems 3730XL following the company's recommendations. Chromatographs were examine with MEGA v7.0.26 (Kumar et al. 2016).

Electron microscopy

Cultures were grown in PmTG broth for one week and then subcultured in 0.22 µm-filtered seawater for three days. Samples were then centrifuged in 50-mL polypropylene tubes at 4,000 x *g* for one hour to pellet material. The samples were then fixed using modified Trumps universal fixative (100mM cacodylate acid, 4% formaldehyde, 1% glutaraldehyde and 2mM MgCl) overnight and rinsed twice for 15-minutes with 0.1M sodium cacodylate buffer. Samples were postfixed in 2% OsO_4 in 0.12M sodium cacodylate buffer for 30-minutes and rinsed twice for 15-minutes with 0.1M sodium cacodylate buffer. Samples were serially dehydrated with ethanol: 30% for 5 minutes, followed by 60%, 90% and 96% for 10 minutes each and finally rinsed in 100% ethanol twice for 10-minutes. After ethanol rinsing, the sample was rinsed with propylene oxide three times for five minutes. Samples were embedded with propylene oxide and epoxy resin (EPON) 1:1 overnight. Samples were left to polymerize at 60 °C for one day. Imaging was conducted with a JEM-1010 electron microscope (JEOL, Tokyo, Japan).

Phylogenetic analysis

Multiple sequence alignments (MSA) were created from DNA sequences retrieved from the NCBI database (Table 1) and subsequently aligned in MEGA7 using Muscle. All unalignable regions were manually removed. MEGA7 was used to identify the best-fit substitution model for phylogenetic tree generation using Bayesian information criterion. A neighbor joining tree was generated and then bootstrapped using maximum likelihood (ML) with 1,000 pseudoreplications. Maximum parsimony (MP) trees were estimated from the MSAs and

bootstrapped following 1,000 pseuoreplications. Maximum Composite Likelihood models were used in MEGA7 to comparatively assess the number of inter and intra-genus base substitutions per site. Our isolate, *L. haliotidis*, and thraustochytrid isolates M4-103 and two AR2-19 sequences were grouped within the *Labyrinthulochytrium* for inter and intra-genetic comparison.

RESULTS

Taxonomy

Labyrinthulochytrium B.T. Hassett et R. Gradinger, gen. nov.

ZooBank: urn:lsid:zoobank.org:pub:B93152E1-7AEF-47FE-BE7C-90697BF9685A

Pinus pollinis consummo et in haliotidae parasitica. Facile ius nutriendum esse colo. Cretacea alba moles; sporangium epibioticum; sporangium vegetativae plerumque sphaeroideon subeo (dia 4.5-14 μm). In ius nutriendum mavultis binarii dividit; in marinis, binarii dividit retard et zoospore productionem amplifico. Zoosporum motorium cum flaggelum duo, ovalibus aliquantum (dia 4.5-12 μm). Mitochondria cristae tubulata continet; interdum, hyoideum informe circum nucleum.

Saprobic on pine pollen and parasitic on abalone. Easily grown on nutrient media. Greyish white to white in mass culture; sporangium epibiotic; vegetative stages usually spheroidal in shape (4.5-14 μm in diameter). In nutrient media preferentially divides by binary division; in seawater, binary division is retarded and zoospore production is heightened. Motile biflagellate zoospores slightly oval (4.5-12 μm in diameter). Mitochondria containing tubular cristae, sometimes horseshoe-shaped around the nucleus. Cell wall scales observed sloughing with electron microscopy. Distinguished from other genera based on molecular inference.

Etymology: *labyrinth* = maze, in recognition of the type phylum; *chytrium* = pot, recognizes the type naming scheme for the thraustochytrids

Type species: *Labyrinthulochytrium haliotidis* (Brower 1986) B. T. Hassett et R. Gradinger comb. nov.

Basionym: Labyrinthuloides haliotidis (Brower 1986) emend Leander et al. 2004 to *Aplanochytrium haliotidis*

Labyrinthulochytrium arktikum B.T. Hassett et R. Gradinger, sp. nov.

ZooBank: urn:lsid:zoobank.org:pub:B93152E1-7AEF-47FE-BE7C-90697BF9685A

Pinus pollinis consummo. Facile ius nutriendum et marinum esse colo. Moles albus; sporangium epibioticum; sporangium vegetativae plerumque sphaeroideon subeo (dia 4.5-14 μm). In ius nutriendum mavultis binarii dividit; in marinis, binarii dividit retard et zoospore productio amplifico. Propagationis binarii dividit et zoosporum (~8) propagationis. Zoosporum motorium cum flaggelum duo, ovalibus (dia 4.5-12 μm) et subfusiformum (lateralis) aliquantum. Zoosporum rapidus verso sub vegetativae incrementum. Productio longus (16 μm) cytoplasmum filum ectoplasmum reticulum fictus. Mitochondria cristae tubulata contineo; interdum, hyoideum informibus circum nucleum. Cellulam murus numerosus corium lamellae contentus, protuberatus numerosus et bothrosomus subitus.

Saprobic on pine pollen. Easily grown and maintained on nutrient media or in seawater. White in mass culture; sporangium epibiotic, vegetative stages usually spheroidal in shape (4.5-14 µm in diameter). Asexual reproduction by binary division and zoospore (~8) release. In nutrient media preferentially divides by binary division; in seawater, binary division is retarded and zoospore production is heightened. Motile biflagellate zoospores slightly oval (4.5-12 µm in diameter) and appear subfusiform in lateral view that can spin rapidly prior to settlement and subsequent development into a vegetative cell. Production of long (16 µm) cytoplasmic threads that can form ectoplasmic nets. Mitochondria containing tubular cristae, sometimes horseshoe-shaped around the nucleus. Cell wall comprised of multilayer (up to 10) electron-dense lamellae that can form multiple protuberances, some forming bothrosomes. Cell wall scales observed sloughing with electron microscopy. Distinguished based on molecular inference, the production of large zoospores, the absence of cell clustering. and the absence of a single zoosporangial rupture during zoospore release. *Etymology*: *arktikos* = of the north, recognizes the location of this isolate

Holotype: Fig. 1 – 2 and GenBank SSU rRNA sequence SUB3113088. Isolated from nearshore seawater, Tromsø, Norway (N69.663 E18.906).

Labyrinthulochytrium haliotidis (Bower 1986) B.T. Hassett et R. Gradinger, comb. nov.

=*Labyrinthuloides haliotidis* (Brower 1986) emend Leander et al. 2004 to *Aplanochytrium haliotidis*

At the time of field collection (22 May 2017) the salinity of seawater was 27.6. After three days of incubation at room temperature, spheroidal sporangia were observed epiphytically attached to pine pollen (Fig. 1A). Sporangia were then transferred onto PmTG agar medium and were observed after several days producing innumerable zoospores. Cells were capable of growing at a temperature range between $4 – 25$ °C. After several iterations of subculturing, axenic cultures were transferred to broth PmTG medium and were observed reproducing by mitosis and less frequently by zoospore production. Vegetative cells were capable of floating and sinking in culture. Floating cells appeared to contain less intercellular content (Fig. 1B) relative to sinking cell (Fig. 1C). Vegetative cells were between 4.5µm and 14µm (Fig. 1C). Division occurred after the loose consolidation of cytoplasmic material, followed by the formation of a cleavage furrows (Fig. 1D), and subsequent binary division into daughter cells (4.5-14.0µm in diameter). Binary division occurred in rapid succession, seemingly initiating interphase of conjoined daughter cells before the termination of cytokinesis. Many cells produced long (~66 µm in length) cytoplasmic threads that moved independently of the sporangium. After binary division, daughter cells generally migrated away from parent cells. Cytoplasmic threads were able to interact to form reticulate ectoplasmic nets (Fig. 1E). Prolonged mitotic division produced an extensive matrix of cells interconnected by their cytoplasmic nets. This extensive matrix could easily be manipulated in broth culture as a biofilm of non-overlapping cells. In general, dense broth cultures smelled strongly of fish. Cells maintained in culture for >1month produced atypically large cells (Fig. 1F) 20-35 µm in diameter.

After binary division in nutrient medium and subsequent transfer to sterile seawater, cells underwent repeated rounds of binary division that, instead of migrating after division, formed a single round cluster of approximately eight associated cells (Fig. 1G). These associated cells remained clustered until some unknown physical mechanism elongated the single round cluster into a more planer cluster of cells (Fig. 1F). Within five minutes of cluster elongation, cells began to sequentially dissociate (Vid. 1) and rapidly migrate. These zoospores ranged in

size (4.5-12 µm in diameter) and possessed two flagella (Fig. 1I, 12µm in length). Zoospores remained motile for several minutes before many rapidly spun (seemingly uncoiling and converting their flagella into the long cytoplasmic threads), then temporarily entered a quiescent state, before resuming normal thread-mediated motility that was typical for mature cells. After this conversion, some newly-formed vegetative cells used their long cytoplasmic threads for motility (Vid. 1, 1:00 at bottom).

To explore the ecology of our isolate, cells were co-cultured with algae (*Chaetoceros socialis*) and a marine fungi (*Penicillium brevicompactum*) and was explored for parasitism. After two hours of co-culturing with algae, our isolates began to migrate towards the algae with their cytoplasmic threads. After ~30 minutes of interaction with cytoplasmic threads, the isolates began to move away from algal cells. After one day, no parasitism was observed. Cells cultured with mycelia of *P. brevicompactum* migrated towards hyphae and localized along hyphal strands (SFigure 1). Sometimes, hyphal strands would swell in proximity to localized cells (SFigure 2). After three day of co-culturing, there was no observable loss of integrity to hyphal strands as a result of this symbiosis.

BLAST query of the isolate's 18S gene identified closest identity (97.5%) to *Aplanochytrium haliotidis* (NCBI accession U21338.1), followed by 94% identity to several undescribed thraustochytrids isolated in Japan (Ueda et al. 2015). To most accurately estimate molecular data within our multiple sequence alignment, MEGA indicated the most appropriate model of DNA substitution was the Tamura-Nei, 93 with rates of substitution estimated by a gamma distribution (TN93+G). The final MSA alignment included 1,467 positions. Neighbor joining, maximum likelihood, and maximum parsimony phylogenies consistently produced tree topologies that grouped our isolate and *A. haliotidis* among the thraustochytrids, branching sister to undescribed isolates (Fig. 2) and basal to the aplanochytrids and *Labyrinthula*. Within our phylogenetic trees (Fig. 2, SFig. 3), all included genera formed well-supported clades; however, *Thraustochytrium* isolates were interspersed. Terminal nodes were consistently supported by higher bootstrap values greater than or equal to 94% and 84% for ML and MP, respectively. Intra-genera pairwise analysis of DNA was 0.0403 base substitutions per site when averaged across all genera (excluding the *Labyrinthulochytrium*). The average difference within the *Labyrinthulochytrium* was 0.028 (STable 1). Comparative inter-genera pairwise analysis of DNA was 0.135 base substitutions per site when averaged across all genera. The average difference between the *Labyrinthulochytrium* and all other groups was 0.112 base substitutions per site (STable 2).

Transmission electron micrographs (Fig. 3) revealed electron dense, multilayered cell walls that in vegetative cells enclosed a single nucleus in proximity to a single Golgi body, horseshoe-shaped mitochondria with tubular cristae (Fig. 3A), and large lipid globules (sometimes several, Fig. 3B). Cell walls formed multilamellate protuberances contiguous with the cell wall that were generally localized at polar ends of the cell (Fig 3C). Electron micrographs captured cells dividing (Fig. 3D, E), with lamellar cell walls separating developing daughter cells, each with a corresponding nucleus (Fig. 3F). Ectoplasmic nets originated at a complex lamellate protuberances (~500nm-1µm in length) in association with a basal electron dense bothrosome (Fig. 3G). Centrioles comprised of nine microtubule triplets (Fig. 3H) with four unknown central elements (Fig. 3I), were also observed.

DISCUSSION

The Labyrinthulea (=Labyrinthulomycota) are cosmopolitan heterotrophs that have historically been divided into morphology-defined taxa. The phylum level classification of this group remains uncertain (e.g. Cavalier-Smith 2017, FioRito et al. 2016); however, because this group is definitively not part of the True Fungi, we preferentially use the naming scheme Labyrinthulea. Phenotypic plasticity, convergent evolution, and taxonomy based on homoplastic traits has confounded systematics that are reflective of natural taxa (Leander et al. 2004, Bongiorni et al. 2005, Damare & Raghukumar 2006). Consequently, molecular phylogenies based on the 18S rRNA small subunit have been used to guide inferences of evolution among the Labyrinthulea (e.g. Damare & Raghukumar 2006, Yokoyama et al. 2007). Within this molecular paradigm, *Aplanochytrium haliotidis* has been phylogenetically problematic, consistently grouping outside the aplanochytrids in numerous molecular studies of the Labyrinthulea (Bongiornia et al. 2005, FioRito et al. 2016), including in our tests of evolutionary hypothesis conducted in this study; however, speculation that the 18S rRNA sequence was derived from a contaminant (Leander & Porter 2001) likely inhibited earlier reclassification of *A. haliotidis*.

In this study, we isolated an unknown unicellular heterotrophic eukaryote with similar life history, ultrastructure, and close molecular identity to *A. haliotidis*; consequently, we surmise that the 18S sequence associated with *A. haliotidis* was likely derived from the original type specimen. This molecular evidence, in conjunction with life history information (i.e. *A. haliotidis* does not produce aplanospores) underscores the classification of *A. haliotidis* as a thraustochytrid. These data support the earlier suppositions made by Bower (1986) when initially describing *Labyrinthuloides haliotidis* (=*Aplanochytrium haliotidis*) as a close relative of the thraustochytrids. Within this new classification scheme, *L. haliotidis* is still unique among the thraustochytrids, as it is capable of reproducing by binary division (a trait that it shares with only two out of the ten described thraustochytrid genera: *Aurantiochytrium* and *Schizochytrium*), is not pigmented, and does not release naked protoplast (Table 2). Our new isolate, represented as *Labyrinthulochytrium artikum,* is readily differentiated from *Labyrinthulochytrium haliotidis* by the production of large zoospores of approximate size to vegetative-dividing cells and the absence of a zoosporangial cell wall during zoospore release (Table 3). The observation of a hyphal swellings and prolonged association of our isolate with *P. brevicompactum* suggests that it may possess virulence-associated properties.

Phylogenetically, our isolates fall among a core group of undescribed thraustochytrids isolated in Japan (Ueda et al. 2015), branching sister to isolates AR2-19 and M4-103. Based on molecular phylogeny, it is possible that *Labyrinthulochytrium* circumscribes these uncharacterized isolates; however, without life history information, we are unable to confidentially include these isolates within the *Labyrinthulochytrium* or concisely describe the evolutionary relationship of this genus without circumscribing other genera. Future characterization of these isolates will elucidate evolutionary relationships among *Labyrinthulochytrium* and its nearest-branching clades. Intra-genus genetic differences among the thruastochytrids (0.0403 base substitutions per site) (STable 1) was greater than the genetic differences within our new genus (0.028 base substitutions per site), suggesting our proposed clade is comprised of more genetically-similar isolates, relative to other genera. Inter-genus genetic differences among the thraustochytrids (0.135 base substitutions per site) was slightly greater than the average distance of our new genus to all other genera (0.112 base substitutions per site); however, our new genus exceeded the average distance of *Botryochytrium* to all other thraustochytrid genera (0.110 base substitutions per site), supporting the uniqueness of our novel genera relative to other recognized clades. The

backbone of our phylogenetic trees was considerably less supported than terminal nodes. To resolve deep-branching relationships and to form robust inferences of evolution, we suggest that future research employ multigene concatenated phylogenies to test the evolutionary relationships within the Labyrinthulea (e.g. Cavalier-Smith et al. 2014, Kang et al. 2016) to resolve enigmatic species complexes and identify true amorphic attributes that correspond to respective clades. Among the basal-branching True Fungi, zoospore ultrastructure has been used extensively to guide systematics (e.g. Wyngaert et al. 2017) and may prove useful, in conjunction with molecular data, to understand evolutionary relationships among the Labyrinthulea.

Electron microscopy of *L. arktikum* revealed typical ultrastructural features associated with the Labyrinthulea. We observed cell walls made of electron-dense lamella, which are typical for the thruastochytrids (Darley et al. 1973; Kumar 1982); numerous electron-dense bothrosomes (Moro et al. 2003; Iwata et al. 2016); horseshoe-shaped, tubular mitochondria (Bower 1986); Golgi bodies, nuclei, and vacuoles (Moss 1985). In several cross sections, we observed centrioles with nine microtubule triplets with four unknown central elements. It is possible that these central elements are microtubules that represent a potentially novel configuration (i.e. 9 + 4); however, it is also possible that this centriole was either an intermediate form, or occurred in the distal lumen - a highly variable region with numerous appearances across various taxa.

This research helps redefine the taxonomically enigmatic *L. haliotidis* that is of ecological importance as a parasite of abalone, while characterizing a novel branch of life among the diverse and well-studied thraustochytrids. The range of temperatures in which we were able to maintain *L. arktikum* suggests that this organism may be ecologically relevant throughout the year and could behave as a parasite when associated with temperature-stressed symbionts. Future research is needed to understand the contributions of the Labyrinthulea to marine carbon cycling and the evolutionary relationship among its clades.

ACKNOWLEDGMENTS

LITERATURE CITED

Bahnweg, G. & Sparrow, F. K. 1974. Four new species of *Thraustochytrium* from Antarctic regions, with notes on the distribution of zoosporic fungi in the Antarctic marine ecosystems. *Am. J. Bot.*, 61:754-766.

Bennett, R. M., Honda, D., Beakes, G. W., & Thines, M. 2017. Labryinthulomycota. *In:* Archibald, J. M., Simpson, A. G. B., Slamovits, C. H. (ed.), The Handbook of the Protists. 2nd ed. Springer International Publishing, Gewerbestrasse. 14:507-542.

Bongiorni, L., Jain, R., Raghukumar, S., & Aggarwal, R. K. 2005. *Thraustochytrium gaertnerium* sp. nov.: a new thraustochytrid stramenopilan protist from mangroves of Goa, India. *Protist*, 156:303-315.

Brower, S. M. 1986. *Labyrinthuloides haliotidis* n. sp. (Protozoa: Labyrinthuomorpha), a pathogenic parasite of small juvenile abalone in a British Columbia mariculture facility. *Can. J. Zool.*, 65:1996-2007.

Cavalier-Smith, T. 2017. Kingdom Chromista and its eight phyla: a new synthesis emphasizing periplastid protein targeting, cytoskeletal and periplastid evolution, and ancient divergences. *Protoplasma*, DOI: 10.1007/s00709-017-1147-3.

Cavalier-Smith, T., Chao, E. E., Snell, E. A., Berney, C., Fiore-Donno, A. M., Lewis, R. 2014. Multigene eukaryote phylogeny reveals the likely protozoan ancestors of opisthokonts (animals, fungi, choanozoans) and Amoebozoa. *Mol. Phylogenet. Evol.*, 81:71-85.

Damare, V., Raghukumar, S. 2006. Morphology and physiology of the marine straminipilan fungi, the aplanochytrids isolated from the equatorial Indian Ocean. *Indian J. Mar. Sci.*, 35:326-340.

Darley, W. M., Porter, D., Fuller, M. S. 1973. Cell wall composition and synthesis via Golgi-directed scale formation in the marine eukaryote, *Schizochytrium aggregatum*, with a note on *Thraustochytrium* sp. *Arch. Mikrobiol.,* 90:89-106.

Doi, K., Honda, D. 2017. Proposal of *Monorhizochytrium globosum* gen. nov., com. nov. (Stramenopiles, Labyrinthulomycetes) for former *Thraustochytrium globosum* based on morphological features and phylogenetic relationships. *Phycol. Res.*, 65:188-201.

FioRito, R., Leander, C., Leander, B. 2016. Characterization of three novel species of Labyrinthulomycota isolated from ochre sea stars (*Pisaster ochraceus*). *Mar. Biol.*, 163:170.

Iwata, I., Kimura, K., Tomura, Y., Motomura, T., Kanae, K., Koike, K., Honda, D. 2016. Bothrosome formation in *Schizochyrium aggregatum* (Labyrinthulomycetes, Stramenopiles) during zoospore settlement. *Protist*, 168:206-219.

Kang, S., Tice, A. K. Spiegel, F. W., Silberman, J. D., Pánek, T., Čepička, I., Kostka, M., Kosakyan, A., Alcântara, D. M., Roger, A. J., Shadwick, L. L., Smirnov. A,, Kudryavstev, A., Lahr, D. J. G, Brown, M. W. 2016. Between a pod and a hard test: the deep evolution of Amoebae. *Mol. Biol. Evol.*, 34:2258-2270.

Kumar, S. R. 1982. Fine structure of the thraustochytrid *Ulkenia amoeboidea*. I. Vegetative thallus and formation of the amoeboid stage. *Can. J. Bot.*, 60:1092-1102.

Kumar, S., Stecher, G., Tamura, K. 2016. MEGA7: Molecular Evolutionary Genetics Analysis version 7.0. for bigger datasets. *Mol. Biol. Evol.*, 33:1870-1874.

Hassett, B. T., López, J. A., Gradinger, R. 2015. Two new species of marine saprotrophic sphaeroformids in the Mesomycetozoea isolated from the sub-Arctic Bering Sea. *Protist*, 166:310-322.

Jones, E .B. G., Alderman, D. J. 1971. *Althornia crouchii* gen. et sp. nov., a marine biflagellate fungus. *Nova Hedwigia*, 21:381-400.

Leander, C. A., Porter, D. 2000. Redefining the genus Aplanochytrium (phylum Labyrinthulomycota). *Mycotaxon*, 76:439-444.

Leander, C. A., Porter, D. 2001. The Labyrinthulomycota is comprised of three distinct lineages. *Mycologia*, 93:459-464.

Leander, C. A., Porter, D., Leander, B. S. 2004. Comparative morphology and molecular phylogeny of aplanochytrids (Labyrinthulomycota). *Eur. J. Protistol.*, 40: 317-328.

Moro, I., Negrisolo, E., Callegara, A., Andreoli, C. 2003. *Aplanochytrium stocchinoi*: a new Labyrinthulomycota from the Southern Ocean (Ross Sea, Antarctica). *Protist*, 154:331-340.

Moss, S. T. 1985. An ultrastructural study of taxonomically significant characters of the Thraustochytriales and the Labyrinthulales. *Bot. J. Linnean Soc.*, 91:329-357.

Sparrow, F. K. 1960. Aquatic Phycomycetes. University of Michigan Press, Ann Arbor.

Tsui, C. K. M., Marshall, W., Yokoyama, R., Honda, D., Lippmeier, J. C., Craven, K. D., Peterson, P. D., Berbee, M. L. 2009. Labyrinthulomycetes phylogeny and its implications for the evolutionary loss of chloroplasts and gain of ectoplasmic gliding. *Mol. Phylogenet. Evol.*, 50:129-140.

Ueda, M., Nomura, Y., Doi, K., Nakajima, M., Honda, D. 2015. Seasonal dynamics of culturable thraustochytrids (Labyrinthulomycetes, Stramenopiles) in estuarine and coastal waters. *Aquatic Microb. Ecol.*, 74:187-204.

White, T., Lee, B., Taylor, J. 1990. Amplification and direct sequencing of fungal ribosomal RNA Genes for Phylogenetics. *In*: Innis, M., Gelfand, D., Sninsky, J., White, T. (ed.) PCR Protocols: A Guide to Methods and Applications. Academic Press, Orlando. 38:315–322.

Wyngaert, S. V. D., Seto, K., Rojas-Jimenez, K., Kagami, M. 2017. A new parasitic chytrid, *Staurastromyces oculus* (Rhizophydiales, Staurastromycetaceae fam. nov.), infecting the freshwater desmid *Staurastrum* sp. *Protist*, 168:392-407.

Yokoyama, R. & Honda D. 2007. Taxonomic rearrangement of the genus *Schizochytrium* sensu lato based on morphology, chemotaxonomic characteristics, and 18S rRNA gene phylogeny (Thrasutochytriaceae, Labyrinthulomycetes): emendation for *Schizochytrium* and erection of *Aurantiochytrium* and *Oblongichytrium* gen. nov. *Mycoscience*, 48: 199-211.

Yokoyama, R., Salleh, B., Honda, D. 2007. Taxonomic rearrangement of the genus *Ulkenia* senu lato based on morphology, chemotaxonomical characteristics, and 18S rRNA gene phylogeny (Thraustochytriaceae, Labyrinthulomycetes): emendation for *Ulkenia* and erection of *Botryochytrium*, *Parietichytrium*, and *Sicyoidochytrium* gen. nov. *Mycoscience*, 48: 329-341.

FIGURE LEGENDS

Fig. 1. Light microscopy of *Labyrinthulochytrium arktikum*. Black scale bar represents 10µm. A) Pine pollen (p) with *L. arktikum* attached epibiotically (white arrow). B) Floating cells recovered by touching a glass coverslip to the surface of the water with less visible cytoplasmic inclusions than sinking cell varieties. C) Representative vegetative cells after several generations of binary division illustrating spacing and variation of size. D) Dividing cells in PmTG media. E) Cells with cytoplasmic threads forming ectoplasmic net, while dividing. F) Large cell after several weeks in culture. G) Cluster of cells formed during zoospore development. H) Cell cluster following elongation and prior to sequential zoospore dispersal. I) Two zoospores, one displaying biflagellation.

Fig. 2. Condensed, rooted phylogenetic tree of unknown and described thraustochytrids with nodes displaying maximum parsimony/maximum likelihood values following 1,000 pseudoreplications. Shaded area illustrates our new species that branches sister to *Labyrinthulochytrium haliotidis*.

Fig. 3. Transmission electron micrographs of *L. arktikum*. A) A representative cross section of a vegetative cell with a nucleus (N) containing a nucleolus (NU), a Golgi body (G) in close proximity to the nucleus, and horseshoe-shaped mitochondria with tubular cristae (M). B) Small vegetative cell filled with four lipid globules in association with a mitochondria. C) Vegetative cell with a lamellar protuberance (LP) comprised of contiguous electron dense strands. D) Cell undergoing binary division with two nuclei, mitochondria, and a newly-formed, electron dense, thin cell wall (CW). E) Diving cell splitting into three section, each section separated by an electron-dense, newly-formed cell wall, electron dense inclusions (EDI) localized to the vacuoles. F) Three completely-cleaved cells enclosed in a contiguous cell wall, each cell with its own nucleus. Also observable is a Golgi body, an electron dense inclusion localized to a vacuole, and a mitochondria. G) Complex lamella protuberance in association with the bothrosome (white arrow). H) Vegetative cell with two lamellar protuberances, one protuberance is in close proximity to a centriole. I) Two centrioles in proximity to a lamellar protuberance. The centriole on the left is comprised of nine microtubule triplets with four unknown central elements.

Table 1. GenBank accession numbers of 18S rRNA loci used to test evolutionary hypotheses.

Table 2. Diagnostic table that details morphological differences between described genera.

Table 3. Summary of morphological differences between *L. haliotidis* and *L. arktikum*.

SUPPORTING INFORMATION

Figure S1. Light microscopy at 400x magnification showing the association of *L. arktikum* along the hyphae of *P. brevicompatcum*.

Figure S2. Light microscopy at 1,000x magnification of *P. brevicompactum* hyphal swellings forming in proximity to localized *L. arktikum* cells.

Figure S3. Expanded phylogenetic tree showing representative genera and the most genetically similar isolates to *L. arktikum* displaying maximum parsimony/maximum likelihood values following 1,000 pseudoreplications.

Table S1. The number of base substitutions per site from averaging over all sequence pairs within each group are shown. Analyses were conducted using the Maximum Composite Likelihood model in MEGA7.

Table S2. The number of base substitutions per site from averaging over all sequence pairs between groups are shown. Analyses were conducted using the Maximum Composite Likelihood model.

Movie S1. Light microscopy video capturing sequential zoospore dispersal and sporangium motility in seawater.

Table 1. GenBank accession numbers of 18S rRNA loci used to test evolutionary hypotheses.

Isolate/Taxon Name	GenBank Accession Numbers
Ingroup:	
Labyrinthulochytrium arktikum	**MG099001**
Aplanochytrium blankum	KX160007.1
Aplanochytrium kerguelense	AB022103.1
Aplanochytrium minuta	L27634.1
Aplanochytrium stocchinoi	AJ519935.1
Aplanochytrium haliotidis	U21338.1
Aplanochytrium sp. SC2129	EU851171.1
Aplanochytrium sp. SC24-1	AF348521.1
Aplanochytrium sp. PR12-3	AF348517.1
Aplanochytrium sp. PR15-1	AF348518.1
Aplanochytrium sp. PR1-1	AF348516.1
Aplanochytrium sp. PBS07	FJ799799.1
Aplanochytrium sp. APKK4	KT901795.1
Aplanochytrium sp. S1a	FJ810216.1
Aplanochytrium sp. SC1-1	AF348520.1
Aplanochytrium sp. S19610	EU851168.1
Aplanochytrium sp. S1961	EU851167.1
Aplanochytrium sp. S2124	EU851169.1
Aplanochytrium sp. S2128	EU851173.1
Aplanochytrium sp. S2125	EU851170.1
Aurantiochytrium sp. RCC893	AB973565.1
Aurantiochytrium limacinum	AB973564.1
Aurantiochytrium sp. 18W	AB811030.1
Aurantiochytrium sp. 18W-15a	AB811029.1
Botryochytrium radiatum	AB355410.1
Botryochytrium profunda	AB022114.1
Botryochytrium radiata	AB022115.1
Botryochytrium sp. 143	DQ023614.1
Labyrinthula sp. L72	AB220158.1
Labyrinthula sp. L59	AB095092.1
Labyrinthula sp. N12	AB246795.1
Labyrinthula sp. N8	AB246794.1
Labyrinthula zosterae	FR875311.2
Parietichytrium sarkarianum	AB244715.1
Parietichytrium sp. MBIC11085	AB290580.1
Parietichytrium sarkarianum	AB355411.1
Parietichytrium sp. F3-1	AB073304.2
Parietichytrium sp. H1-14	AB073305.2
Thraustrochytrium sp. AR2-19	AB810952.1
Thraustochytrium sp. AR2-19	AB810950.1
Thraustochytriidae sp. SEK 691	AB973546.1
Thraustochytriidae sp. SEK 690	AB973545.1
Thraustochytriidae sp. SEK 692	AB973547.1
Thraustochytriidae sp. M4-103	AB073307.1
Thraustochytrium aureum	AB022110.1

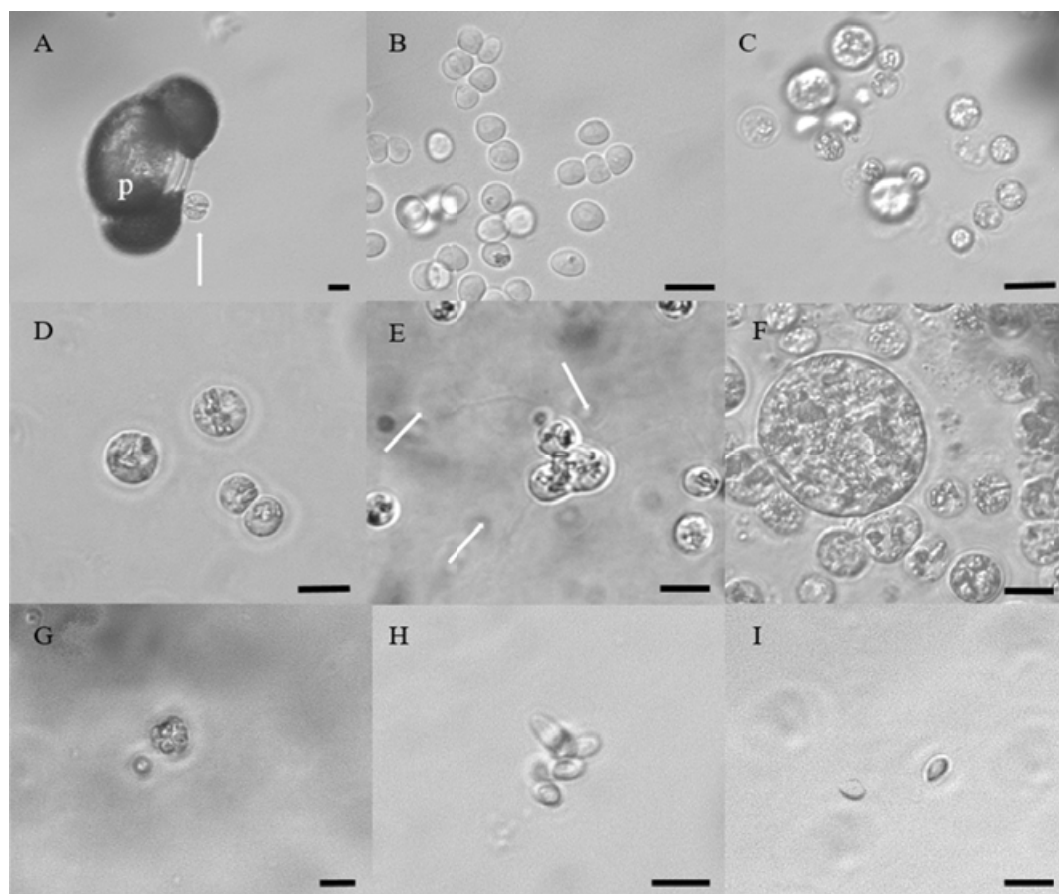|	
Thraustochytrium kinnei	L34668.1
Thraustochytrium gaertnerium	AY705753.2
Thraustochytrium aggregatum	AB022109.1
Thraustochytrium pachydermum	AB022113.1
Thraustochytrium striatum	KT598545.1
Thraustochytrium striatum	AB022112.1
Schizochytrium sp.	AB052556.1
Schizochytrium aggregatum	AB022106.1
Schizochytrium sp. SEK 210	AB290576.1
Schizochytrium sp. SEK 346	AB290578.1
Schizochytrium sp. SEK 345	AB290577.1
Sicyoidochytrium minutum	AB355412.1
Sicyoidochytrium sp.	AB183659.1
Sicyoidochytrium minutum	AB290585.1
Ulkenia sp. SEK 214	AB290355.1
Ulkenia sp. ATCC28207	AB022104.1
Ulkenia visurgensis	AB022116.1
Ulkenia visurgensis 141	DQ100296.1
Ulkenia profunda	L34054.1
Outgroup:	
Chromera velia	JN986791.1
Heterocapsa triquetra	GU594638.1
Euplotidium arenarium	Y19166.1

Table 2. Diagnostic table that details morphological differences between described genera.

	Pigmented thallus	Binary division	Protoplast release	Reference
Althornia		No		Jones & Alderman 1971
Aurantiochytrium	Yes			Yokayama & Honda 2007
Botryochytrium		No		Yokayama et al. 2007
Japonochytrium		No		Sparrow 1960
Labyrinthulochytrium	**No**	**Yes**	**No**	-
Monorhizochytrium		No		Doi & Honda 2017
Parietichytrium		No		Yokayama et al. 2007
Schizochytrium	Yes			Yokayama et al. 2007
Sicyoidochytrium		No		Yokayama et al. 2007
Thraustochytrium		No[1]		Doi & Honda 2017
Ulkenia		No	Yes	Yokayama et al. 2007

[1]*Thraustochytrium aggregatium* is the only exception

Table 3. Summary of morphological differences between *L. haliotidis* and *L. arktikum*.

	Forms clusters	Zoospore diameter	Binary division	Zoosporangial rupture
L. haliotidis	Yes	3.7-7.1 µm	Yes	Yes
L. arktikum	No	4.5-12 µm	Yes	No